Published in final edited form as:
*Arterioscler Thromb Vasc Biol*. 2011 January ; 31(1): 102–109. doi:10.1161/ATVBAHA.110.216036.

# Matrix metalloproteinase activation predicts amelioration of remodeling following dietary modification in injured arteries

**Sina Tavakoli**, **Mahmoud Razavian**, **Jiasheng Zhang**, **Lei Nie**, **Ravi Marfatia**, **Lawrence W. Dobrucki**, **Albert J. Sinusas**, **Simon Robinson**, **D. Scott Edwards**, and **Mehran M. Sadeghi**
Cardiovascular Molecular Imaging Laboratory, Section of Cardiovascular Medicine (S.T., M.R., J.Z., L.N., R.M., L.W.D., A.J.S., M.M.S.), Yale University School of Medicine, New Haven, CT; VA Connecticut Healthcare System (S.T., M.R., J.Z., L.N., R.M., M.M.S.), West Haven, CT; Lantheus Medical Imaging (S.R., D.S.E.), North Billerica, MA

## Abstract

**Objective—**To establish and validate early non-invasive imaging of matrix metalloproteinase (MMP) activation for monitoring the progression of vascular remodeling and response to dietary modification.

**Methods and Results—**Apolipoprotein $E^{-/-}$ mice that were fed a high fat diet underwent left common carotid artery wire injury. One week after surgery, a group of animals were withdrawn from the high fat diet. The other group of animals continued that diet throughout the study. MicroSPECT/CT imaging with RP805 (a $^{99m}$Tc-labeled tracer targeting activated MMPs) was repeatedly performed at 2 and 4 weeks after surgery. Histological analysis at 4 week showed significant left carotid neointima formation, monocyte/macrophage infiltration, and upregulation of several MMPs, which were ameliorated by withdrawal from the high fat diet. In vivo microSPECT/CT images visualized significant RP805 uptake, reflecting MMP activation, in the injured carotid arteries. MMP activation was reduced as early as 1 week after withdrawal from the high fat diet and significantly correlated with neointimal area at 4 weeks after surgery.

**Conclusion—**MMP activation predicts the progression of vascular remodeling and can track the effect of dietary modification following vascular injury.

### Keywords

vascular remodeling; matrix metalloproteinases; dietary modification; inflammation

Despite recent preventive, diagnostic, and therapeutic advances, cardiovascular diseases remain a major cause of mortality worldwide. Vascular remodeling, changes in the vessel wall geometry and structure, contributes to the pathogenesis of many vascular diseases, including atherosclerosis, post-angioplasty restenosis and aneurysm. A number of preventive and therapeutic measures (e.g., smoking cessation and controlling hypertension and hyperlipidemia) aim at changing the natural course of vascular remodeling [1]. Early monitoring of the effects of these measures may potentially enhance their effectiveness by providing the opportunity to personalize interventions. Conventional imaging modalities

Corresponding author: Mehran M. Sadeghi, VA Connecticut Healthcare System, 950 Campbell Ave., West Haven, CT 06516. mehran.sadeghi@yale.edu.

**Disclosure**
Simons Robinson and D. Scott Edwards are employees of Lantheus Medical Imaging. Albert J. Sinusas and Mehran M. Sadeghi receive experimental tracers from Lantheus Medical Imaging. Albert J. Sinusas has received research grants from Lantheus Medical Imaging.

(e.g., angiography, MRI and perfusion imaging) provide valuable anatomical and physiological information for patient care. However they cannot detect early biological processes that precede the development of advanced vascular diseases. Molecular imaging is a potentially powerful strategy for early detection of vascular remodeling which may also help predict the natural course of the disease and its response to therapy.

Matrix metalloproteinases (MMPs) contribute to a variety of physiological and pathological processes, including wound healing, inflammation, angiogenesis, cancer metastasis and vascular remodeling [2, 3]. MMP activity is delicately controlled at transcriptional and post-transcriptional (activation) levels, as well as by the presence of inhibitors such as tissue inhibitors of matrix metalloproteinases (TIMPs) [4, 5]. Several MMPs, including MMP-2 and MMP-9, are upregulated in remodeling arteries and play key roles in the remodeling process [2]. Recent development of $^{111}$In-labeled RP782 and its homologue, $^{99m}$Tc-labeled RP805 that specifically target the MMP activation epitope has provided an opportunity to image and quantify MMP activation by scintigraphic imaging in vivo in cardiovascular pathologies [6, 7]. Using this approach, it was shown that MMP activation is enhanced in the remodeling left ventricle following myocardial infarction [6]. We have previously reported that MMPs are activated following wire injury in carotid arteries of apolipoprotein E (apoE) deficient mice and their activation can be detected and quantified by MMP-targeted microSPECT/CT imaging in vivo [7]. Here, we extend the scope of those findings to demonstrate that MMP activation in injured arteries detected by molecular imaging using RP805 is: a) reduced as early as one week after a potential therapeutic intervention, i.e., dietary modification; and b) can track and predict the effect of this intervention on vascular remodeling at a later time point. Interestingly, there is a correlation between the presence of macrophages and MMP-2, -3, -12, and -13, but not MMP-9, expression in remodeled arteries.

## Methods

### Animal Model

Animal experiments were performed according to regulations of Yale University and West Haven VA's Animal Care and Use Committees. Left common carotid artery remodeling was induced in apoE$^{-/-}$ mice, as described [7]. Briefly, 8–10 week old female apoE$^{-/-}$ mice (Jackson Laboratory, Bar Harbor, ME) were fed with a high fat diet (TD 88137, 21% anhydrous fat by weight, Harlan-Teklad, Madison, WI). One week later, animals were anesthetized via intra-peritoneal administrations of ketamine (100 mg/kg) and xylazine (10 mg/kg). Common carotid and external carotid arteries were exposed by blunt-end dissection and the left common carotid artery was injured by 3 passes of a 0.014-inch guidewire introduced through the external carotid artery. Right carotid arteries underwent sham operation and served as controls. Postoperative analgesia was achieved by adding ibuprofen (0.11 mg/ml) to drinking water for 3 days. One week after surgery, a group of animals was withdrawn from high fat diet (withdrawal group). The other group was continuously fed with the high fat diet (high fat diet group).

### MicroSPECT/CT Imaging

RP805, a $^{99m}$Tc-labeled tracer with specific binding to the activated catalytic domain of several MMPs [6], was provided by Lantheus Medical Imaging (North Billerica, MA). It is a macrocyclic compound developed on the basis of the structures of known MMP inhibitors and has a MMP-binding portion similar to $^{111}$In-labeled RP782 [6]. Its specificity for MMP-2 was demonstrated using several known MMP inhibitors [6]. The Ki values of the precursor for various activated MMPs are reported as follows: MMP-2, 10.5 nmol/L; MMP-3, 14 nmol/L; MMP-7,<6.4 nmol/L; MMP-9, 7.4 nmol/L; MMP-12, <6 nmol/L; andMMP-13, 7.3 nmol/L [6]. Animals were serially imaged at 2 (N= 7 in each group) and 4 weeks following carotid

injury (1 and 3 weeks after dietary modification, respectively) using a high-resolution small animal imaging system (X-SPECT, Gamma Medica-Ideas, Northridge, CA) with low-energy 1-mm pinhole collimators two hours after intravenous (right jugular vein) administrations of RP805 (40.8 ± 1.3 MBq). Images could not be obtained from two animals in the high fat diet group that expired during the second imaging. Anesthetized mice (under isoflurane) were placed in a fixed position on the animal bed. Three point sources of known activities (37 to 185 kBq) were placed in the field of view to verify the accuracy of image fusion. MicroSPECT images were acquired using the following parameters: 360 degrees, 128 projections, 30 seconds/projection (~80 minute image acquisition), matrix 82 × 82, with 140 keV photopeaks ± 10% window. The diameter of the effective field of view at 4.5 cm radius of rotation was ~5cm [8]. The spatial resolution in tomographic images with a 1mm pinhole collimator for $^{99m}$Tc was 1.1 to 1.2 mm Full-Width Half Maximum (FWHM) and the pixel size for the detector was 1.5 mm with images magnified 1.3-fold at this radius of rotation [8]. After the completion of microSPECT images, the animals were injected with Fenestra (200 μl, Advanced Research Technologies, Montreal, QC, Canada) and CT imaging was performed (energy 75 kVp/280 μA, matrix 512x512) to identify anatomic structures. Compared to the microSPECT system, the CT system has a larger field of view with a spatial resolution of ~50μm. MicroSPECT images were reconstructed by iterative reconstruction using system software (X-Flex) developed by the manufacturer. CT projection images were reconstructed with commercial software (Cobra, Exxim Computing Corp, Pleasanton, CA) that implements a cone-beam reconstruction algorithm. Reconstructed microSPECT images were reoriented according to the CT anatomic images, fused, and exported in the Interfile format for further processing with Amide's Medical Imaging Data Examiner. For quantitative analysis of tracer uptake, cylindrical regions of interest (2×2×2 mm) were drawn at the level of carotid artery bifurcation. A region of interest immediately posterior to both carotids (2×2×2 mm) served as background. Background-corrected values were used to compare tracer uptake of the vessels. The residual blood pool activity was measured in regions of interest drawn over the heart.

### Histology, Morphometry, Immunofluorescent Staining and Zymography

After the last imaging experiments, carotid arteries were harvested and embedded in OCT compound for histomorphometrical analysis. Hematoxylin and eosin staining was performed on 5-μm-thick cryostat sections following standard protocols. Morphometric measurements were performed using NIH ImageJ software (National Institutes of Health, Bethesda, MD), as described [9]. Immunostaining was performed according to standard protocols using the following primary antibodies: anti-mouse MMP-2, MMP-3, MMP-9, MMP-12 and MMP-13 (Santa Cruz Biotechnology, Santa Cruz, CA), and anti-mouse macrophage (F4/80, Abcam, Cambridge, MA). Isotype-matched antibodies served as negative controls. Cy3-conjugated secondary antibodies were used to detect MMP expression. F4/80 was detected with biotin-labeled goat anti-rat IgG (Kirkegaard & Perry Laboratories, Gaithersburg, MD) followed by Alexa 594 Streptavidin (Invitrogen, Carlsbad, CA). Nuclei were counterstained with DAPI (Invitrogen, Eugene, OR). In situ gelatinase zymography was performed using Enz-Check Gelatinase Assay Kit (Molecular Probes). Briefly, 5-mm-thick frozen sections were incubated with buffer in the presence or absence of MMP inhibitor (10 mM 1,10-phenanthroline) for 15 min at 37 °C. Next, DQ gelatin solution (0.1 mg/mL in 1% low melt agar in phosphate-buffered saline; Molecular Probes) and DAPI were added, and the sections were incubated at 37 °C for 60 min. The slides were photographed using a fluorescent microscope equipped with a digital camera.

### Quantitative Reverse Transcription Polymerase Chain Reaction (qRT-PCR)

Total RNA was isolated from carotid arteries using Absolutely RNA® Nanoprep Kit (Stratagene, La Jolla, CA), and reverse transcribed using QuantiTect® Reverse

Transcription Kit (QIAGEN, Valencia, CA) according to manufacturers' instructions. qRT-PCR was performed on cDNA in triplicates using Taqman® gene expression assays (Applied Biosystems, Foster City, CA) and an Applied Biosystems 7500 Real-Time PCR System. The specificity of PCR amplification was confirmed by running PCR products on agarose gels. The results were normalized to glyceraldehyde 3-phosphate dehydrogenase (GAPDH). Two samples which could not be used due to technical issues and outliers were excluded from qRT-PCR analysis. The following primer sets were used: MMP-2, (Mm00439506_m1), MMP-3, (Mm00440295_m1), MMP-9, (Mm00442991_m1), MMP-12, (Mm00500554_m1), MMP-13, (Mm01168713_m1), CD68 (Mm00839636_g1), epidermal growth factor module-containing mucin-like receptor 1 (EMR1, Mm00802529_m1) and GAPDH (Mm99999915_g1)

### Statistical Analysis

Data are expressed as mean ± standard error of the mean. Analysis of variance (ANOVA) followed by Tukey's post-hoc test were used to compare the mean values for multiple groups. A paired *t* test was used to examine the statistical significance ofthe differences in tracer uptake of individual animals at 2 and 4 weeks after surgery. Pearson's correlation analysis was performed to examine the correlation between pairs of parameters. $P < 0.05$ was considered statistically significant.

## Results

### Dietary Modification and MMP Activation in Carotid Artery Remodeling

We have previously reported that mechanical injury to carotid arteries in apoE$^{-/-}$ mice fed a high fat diet leads to significant expansive remodeling and neointima formation over a period of 4 weeks [7]. This remodeling process is associated with enhanced MMP activation and can be non-invasively detected by MMP-targeted microSPECT imaging in vivo [7]. To investigate the effect dietary modification on injury-induced MMP activation, a group of high fat-fed apoE$^{-/-}$ mice were placed on normal chow one week after left common carotid artery mechanical injury (withdrawal group, Figure 1A). The high fat diet was continued in another group of animals (high fat diet group). One week later (2 weeks after left carotid injury), microSPECT/CT imaging with RP805, a $^{99m}$Tc-labeled tracer with specificity for activated MMPs [6], showed focal uptake of RP805 in the injured left carotid artery (Figure 1B). This signal appeared less intense in the withdrawal group. Quantification of in vivo RP805 uptake demonstrated a significant increase in background-corrected RP805 uptake in injured left, compared to sham-operated right carotid arteries in both groups of animals (Figure 1C). RP805 uptake in the injured left carotid artery was significantly reduced in the withdrawal group (high fat diet: 0.43 ± 0.03 counts/voxel/MBq injected *vs* withdrawal: 0.30 ± 0.05 counts/voxel/MBq injected, $P < 0.05$, Figure 1C). The residual blood pool activity measured in a region of interest drawn over the heart was similar between the high fat diet and withdrawal groups of animals (supplemental Figure I), indicating that the observed difference in carotid uptake is not secondary to different tracer clearance kinetics. Similar results were obtained on repeat microSPECT/CT imaging in the same animals at 4 weeks after injury (3 weeks after dietary modification, Figure 1D). Furthermore, repeat RP805 microSPECT/CT imaging showed the persistence of left carotid tracer uptake in animals fed with the high fat diet (0.43 ± 0.03 counts/voxel/MBq injected at two weeks *vs* 0.39 ± 0.06 counts/voxel/MBq injected at four weeks, *P*: N.S.). Withdrawal from the high fat diet led to a significant reduction in left carotid RP805 uptake on repeat images (0.30 ± 0.05 counts/voxel/MBq injected at two weeks *vs* 0.21 ± 0.04 counts/voxel/MBq injected at four weeks, $P < 0.05$). There was also a statistically non significant trend toward reduction in the right carotid artery RP805 uptake following withdrawal from the high fat diet.

### The Effect of Dietary Modification on Indices of Remodeling and Inflammation

Withdrawal from the high fat diet led to significant reduction in non-fasting plasma total cholesterol level (high fat diet: 1926 ± 109 mg/dl *vs* withdrawal: 729 ± 60 mg/dl, $P< 0.001$). As expected, left carotid artery injury in animals fed with the high fat diet resulted in remarkable neointima formation and expansive remodeling of the vessels over a period of 4 weeks (Figure 2A). Early withdrawal from the high fat diet after injury significantly ameliorated the remodeling process with the neointimal cross-sectional area decreasing from 0.076 ± 0.010 $mm^2$ in the high fat diet group to 0.041 ± 0.010 $mm^2$ in the withdrawal group ($P< 0.05$, Figure 2A and B). There was also a trend toward reduction in the total vessel area which did not reach statistical significance.

Monocyte-derived macrophages are important sources of MMP production in the vessel wall [2], and the enhanced monocyte-macrophage recruitment associated with hyperlipidemia may be, at least in part, responsible for the exaggerated vascular remodeling in animals fed with a high fat diet. As expected, F4/80 immunostaining demonstrated the presence of macrophages in remodeled arteries (supplemental Figure II). We investigated the effect of dietary modification on monocyte-macrophage recruitment by qRT-PCR. CD68, a routinely used marker, reflects the presence of phagocytic activity and can be induced by cholesterol-loading in VSMCs [10]. EMR1 (F4/80 antigen) is a more specific marker of mouse macrophages [11]. There was a strong correlation between CD68 and EMR1 expression quantified by qRT-PCR in the injured and sham-operated carotid arteries ($R=0.83$, $P< 0.001$). GAPDH-normalized expression of both CD68 and EMR1 was significantly increased in injured left carotid arteries as compared to sham-operated right carotid arteries in high fat fed animals ($P< 0.01$, Figure 2C–D). Early withdrawal from the high fat diet was associated with a 42% and 52% (albeit not statistically significant) reduction in CD68 and EMR1 expression in injured left carotid arteries (Figure 2C–D).

### MMP Expression in Injury-Induced Vascular Remodeling

Next, we investigated the expression of several MMP targets of RP805 in sham-operated and remodeling arteries at 4 weeks after carotid injury. In sham-operated right carotid arteries of high fat fed mice, expression of MMP-2 (mainly in the adventitia), MMP-9 (mainly in the media), and MMP-12 (in both media and adventitia) were readily detectable, while little MMP-3 and MMP-13 could be detected by immunostaining (Figure 3A). In remodeling arteries, MMP-2, MMP-3, MMP-9, MMP-12 and MMP-13 were diffusely expressed and predominantly localized in the neointima and media (Figure 3A). This diffuse expression prohibited the accurate co-localization of MMPs with specific cells in the vessel wall. Similar results were obtained in the withdrawal group (supplemental Figure IIIA). MMP activity of carotid arteries was assessed by in situ gelatinase zymography at 4 weeks after surgery (Fig. 3B). In the high fat diet group of animals, protease activity was present in a diffuse pattern in the neointima and media of the injured carotid arteries, whereas minimal activity was detected in the adventitia. The protease activity was markedly lower in the sham-operated arteries. The MMP specificity of protease activity was demonstrated in the presence of an MMP inhibitor, 1,10-phenanthroline. A similar pattern protease activity was detected in the withdrawal group (supplemental Figure IIIB).

Considering the non-quantitative nature of immunostainings and in situ zymography, the effect of dietary modification on MMP expression in vascular remodeling was further assessed with qRT-PCR. In animals fed with the high fat diet, GAPDH-normalized mRNA expression of MMP-2, MMP-3, MMP-12 and MMP-13 was significantly higher in remodeling carotid arteries as compared to the sham-operated vessels (Figure 4). Only MMP-12 remained significantly higher in the injured artery in the withdrawal group. Withdrawal from the high fat diet was associated with a significant decrease in MMP-2,

MMP-3 and MMP-13, expression in injured arteries (Figure 4). Consistent with the role of monocyte-macrophages as major sources of MMP production in vascular remodeling, there were significant correlations between CD68 and EMR1 with MMP-2, MMP-3, MMP-12 and MMP-13 mRNA expression in the vessel wall (supplemental Table). RP805 uptake (reflecting global MMP activation) in carotid arteries at 4 weeks after injury significantly correlated with MMP-2, MMP-3, and MMP-13, CD68, as well as EMR1 mRNA expression (Table 1).

### MMP Activation and Prediction of Outcome in Vascular Remodeling

Early MMP activation can potentially predict the course of vascular remodeling and response to dietary modification in individual subjects. Therefore, we investigated whether there is a correlation between MMP activation assessed by RP805 imaging at 2 weeks and indices of remodeling at 4 weeks after injury. We found a strong correlation between background-corrected RP805 uptake of injured carotid arteries at 2 weeks, and neointimal cross-sectional area at 4 weeks after injury (Figure 5; R=0.79, $P< 0.001$), indicating that early assessment of MMP activation by molecular imaging can predict the outcome in vascular remodeling.

## Discussion

The feasibility of detection and quantification of MMP-activation by molecular imaging has been previously demonstrated in animal models of vascular remodeling [7, 12–16]. In this study, we used non-invasive molecular imaging of MMP activation to obtain quantitative in vivo information on the course of injury-induced vascular remodeling and response to dietary modification.

MMPs are a group of over 20 zinc-dependant endopeptidases that through their proteolytic activity play an important role in extracellular matrix remodeling [2]. Most MMPs are secreted as inactive pro-enzymes and their activity is delicately regulated by proteolytic cleavage of pro-enzymes, as well as the expression of a group of natural inhibitors known as TIMPs [2, 5]. Up-regulation and activation of MMPs, in particular gelatinases (MMP-2 and MMP-9), by vascular smooth muscle, endothelial and inflammatory cells are key pathologic processes in many cardiovascular diseases, including atherosclerosis [17], aneurysm [18, 19] and ventricular remodeling [20, 21]. Here, we demonstrate that mechanical injury of the carotid artery results in up-regulation of several MMPs, including gelatinase (MMP-2), collagenase (MMP-13), stromelysin (MMP-3), and metalloelastase MMPs (MMP-12). While MMP-9 clearly plays an important role in the pathogenesis of vascular remodeling [19, 22, 23], we did not detect any change in GAPDH-normalized MMP-9 mRNA expression. Our finding is consistent with a previous report that MMP-9 activity returns to the baseline level within 2 weeks after mechanical injury of arteries [24]. MMP-2, MMP-3 and MMP-13 expression levels at 4 weeks correlated well with infiltration of macrophages in the vessel wall, suggesting that they play a persistent role in the remodeling process. Although much of MMP expression and activity was detected in the neointima and media of injured arteries, adventitial inflammation plays an important role in the pathogenesis of atherosclerosis and vascular remodeling [25], and probably contributes to the increased uptake of the injured vessels.

A number of therapeutic interventions have aimed at reducing inflammation and ameliorating the imbalanced MMP activity in cardiovascular disease. Several pharmacologic MMP inhibitors have been developed and evaluated, with limited success, in pre-clinical and clinical trials [26, 27]. Lipid reduction, whether through dietary modification or pharmacological intervention, is a cornerstone of modern preventive and therapeutic approach to vascular diseases [1]. Little is known about the effect of dietary modification on

vessel wall biology. Although the small size of murine carotid arteries precluded the measurement of MMP protein levels or assessment of MMP activity by gel zymography, we show that mRNA expression of members of different classes of MMPs including MMP-2, MMP-3 and MMP-13 (but not MMP-9 or MMP-12) is significantly reduced by withdrawal from high fat diet in remodeling arteries. The selective non-reversal of the effect of dietary modification on MMP-12 expression induced by mechanical injury in the vessel wall is an intriguing unexpected finding. It is reasonable to hypothesize that this non-reversal reflects some form of ongoing changes in the structure or composition of arteries, e.g., healing, in these animals.

Targeting individual members of the MMP family, especially the highly retained members such as MMP-3 and MMP-7, is an intriguing and potentially promising molecular imaging approach to vascular remodeling. In the absence of tracers targeting specific members, targeted imaging of MMP proteolytic activity, rather than merely their abundance, in the vessel wall and elsewhere has been successfully performed using activatable near infrared fluorescent or multimodality probes [28–31] and radiotracers targeted at the exposed catalytic site of activated MMPs (e.g.$^{99m}$Tc-labeled RP805) [7, 12, 13, 32]. While non-invasive application of optical imaging is potentially limited by light photons' restricted depth of penetration, this is not a limitation for scintigraphic imaging of MMPs activation with this family of radiotracers which has shown promising results in a variety of cardiovascular disease such as post-myocardial infarction remodeling [6], and atherosclerosis [12, 13]. Uptake specificity of RP782 and RP805 has been previously demonstrated using excess of non-labeled precursor and a specific MMP inhibitor which inhibited tracer uptake in remodeling arteries [7, 12–16]. The effect of dietary modification on MMP activation at 1 month was previously demonstrated by ex vivo gamma-well counting in a rabbit model of atherosclerosis [12]. However, the ex vivo nature of the quantification method precluded the possibility of serial assessment of MMP activation in the same animal. Using high-resolution microSPECT imaging followed by CT angiography, we have previously shown that MMP tracer uptake in injured carotid arteries can be clearly visualized and distinguished from uptake in surrounding tissues and surgical wound. Quantification of uptake in vivo may be affected by several factors, including partial volume and scatter [33], and these effects may be more prominent in areas of lesser uptake. However, we have previously shown that using this approach the tracer uptake quantified on in vivo images parallels the uptake quantified by autoradiography, including in non-injured arteries which have lower activity [7]. Previous work has also demonstrated a strong correlation between tracer uptake and MMP activity quantified by zymography [7]. Here, we optimized this approach to evaluate the early response to a therapeutic or preventive measure and correlate it with the outcome by serial imaging in the same animal. We show that as early as 1 week after withdrawal from the high fat diet, MMP activation in injured carotid arteries is significantly reduced compared to animals who continued the high fat diet. This would indicate that changes in MMP activation occur rather soon after dietary modification. The dietary modification-induced reduction in MMP activation continues throughout the follow-up period, while MMP activation remains constantly elevated in animals fed with the high fat diet.

In addition to tracking the effect of an intervention in a group of subjects, molecular imaging provided an opportunity to establish whether early MMP activation in individual subjects can provide information on the ultimate course of vascular remodeling. While ex vivo quantification of MMP targeted tracer uptake has been previously shown to correlate with atherosclerotic plaque inflammation and gelatinases expression on cross-sectional studies [12, 13], we demonstrate here that early quantification of MMP activation detected by in vivo microSPECT imaging (2 weeks after surgery) strongly correlates with the late pathological outcome (4 weeks after surgery) manifested as neointima formation. This implies that MMP

activation may reflect, and be targeted to evaluate, the inflammatory status of the vessel wall. As such, if validated in humans, MMP targeted imaging may provide a unique tool for tracking the underlying pathologic processes and help personalize preventive and therapeutic interventions in vascular remodeling.

## Supplementary Material

Refer to Web version on PubMed Central for supplementary material.

## Acknowledgments

**Sources of Funding**

This work is supported by the National Institutes of Health R01HL085093, P01HL70295 and a Department of Veterans Affairs Merit Award to Mehran M. Sadeghi; and a postdoctoral fellowship award from the American Heart Association, 0826025D, to Sina Tavakoli.

## References

1. Lloyd-Jones DM, Hong Y, Labarthe D, Mozaffarian D, Appel LJ, Van Horn L, Greenlund K, Daniels S, Nichol G, Tomaselli GF, Arnett DK, Fonarow GC, Ho PM, Lauer MS, Masoudi FA, Robertson RM, Roger V, Schwamm LH, Sorlie P, Yancy CW, Rosamond WD. Defining and setting national goals for cardiovascular health promotion and disease reduction: the American Heart Association's strategic Impact Goal through 2020 and beyond. Circulation 121:586–613. [PubMed: 20089546]
2. Galis ZS, Khatri JJ. Matrix metalloproteinases in vascular remodeling and atherogenesis: the good, the bad, and the ugly. Circ Res 2002;90:251–262. [PubMed: 11861412]
3. Egeblad M, Werb Z. New functions for the matrix metalloproteinases in cancer progression. Nat Rev Cancer 2002;2:161–174. [PubMed: 11990853]
4. Spinale FG. Myocardial matrix remodeling and the matrix metalloproteinases: influence on cardiac form and function. Physiol Rev 2007;87:1285–1342. [PubMed: 17928585]
5. Visse R, Nagase H. Matrix metalloproteinases and tissue inhibitors of metalloproteinases: structure, function, and biochemistry. Circ Res 2003;92:827–839. [PubMed: 12730128]
6. Su H, Spinale FG, Dobrucki LW, Song J, Hua J, Sweterlitsch S, Dione DP, Cavaliere P, Chow C, Bourke BN, Hu XY, Azure M, Yalamanchili P, Liu R, Cheesman EH, Robinson S, Edwards DS, Sinusas AJ. Noninvasive targeted imaging of matrix metalloproteinase activation in a murine model of postinfarction remodeling. Circulation 2005;112:3157–3167. [PubMed: 16275862]
7. Zhang J, Nie L, Razavian M, Ahmed M, Dobrucki LW, Asadi A, Edwards DS, Azure M, Sinusas AJ, Sadeghi MM. Molecular imaging of activated matrix metalloproteinases in vascular remodeling. Circulation 2008;118:1953–1960. [PubMed: 18936327]
8. Hwang, AB. PhD Dissertation. University of California; San Francisco: 2006. Quantitative imaging in small animals using SPECT-CT.
9. Sadeghi MM, Krassilnikova S, Zhang J, Gharaei AA, Fassaei HR, Esmailzadeh L, Kooshkabadi A, Edwards S, Yalamanchili P, Harris TD, Sinusas AJ, Zaret BL, Bender JR. Detection of injury-induced vascular remodeling by targeting activated alphavbeta3 integrin in vivo. Circulation 2004;110:84–90. [PubMed: 15210600]
10. Rong JX, Shapiro M, Trogan E, Fisher EA. Transdifferentiation of mouse aortic smooth muscle cells to a macrophage-like state after cholesterol loading. Proc Natl Acad Sci U S A 2003;100:13531–13536. [PubMed: 14581613]
11. Khazen W, M'Bika JP, Tomkiewicz C, Benelli C, Chany C, Achour A, Forest C. Expression of macrophage-selective markers in human and rodent adipocytes. FEBS Lett 2005;579:5631–5634. [PubMed: 16213494]
12. Fujimoto S, Hartung D, Ohshima S, Edwards DS, Zhou J, Yalamanchili P, Azure M, Fujimoto A, Isobe S, Matsumoto Y, Boersma H, Wong N, Yamazaki J, Narula N, Petrov A, Narula J.

Molecular imaging of matrix metalloproteinase in atherosclerotic lesions: resolution with dietary modification and statin therapy. J Am Coll Cardiol 2008;52:1847–1857. [PubMed: 19038682]

13. Ohshima S, Petrov A, Fujimoto S, Zhou J, Azure M, Edwards DS, Murohara T, Narula N, Tsimikas S, Narula J. Molecular imaging of matrix metalloproteinase expression in atherosclerotic plaques of mice deficient in apolipoprotein e or low-density-lipoprotein receptor. J Nucl Med 2009;50:612–617. [PubMed: 19289429]
14. Lancelot E, Amirbekian V, Brigger I, Raynaud JS, Ballet S, David C, Rousseaux O, Le Greneur S, Port M, Lijnen HR, Bruneval P, Michel JB, Ouimet T, Roques B, Amirbekian S, Hyafil F, Vucic E, Aguinaldo JG, Corot C, Fayad ZA. Evaluation of matrix metalloproteinases in atherosclerosis using a novel noninvasive imaging approach. Arterioscler Thromb Vasc Biol 2008;28:425–432. [PubMed: 18258820]
15. Amirbekian V, Aguinaldo JG, Amirbekian S, Hyafil F, Vucic E, Sirol M, Weinreb DB, Le Greneur S, Lancelot E, Corot C, Fisher EA, Galis ZS, Fayad ZA. Atherosclerosis and matrix metalloproteinases: experimental molecular MR imaging in vivo. Radiology 2009;251:429–438. [PubMed: 19224894]
16. Schafers M, Riemann B, Kopka K, Breyholz HJ, Wagner S, Schafers KP, Law MP, Schober O, Levkau B. Scintigraphic imaging of matrix metalloproteinase activity in the arterial wall in vivo. Circulation 2004;109:2554–2559. [PubMed: 15123523]
17. Galis ZS, Sukhova GK, Lark MW, Libby P. Increased expression of matrix metalloproteinases and matrix degrading activity in vulnerable regions of human atherosclerotic plaques. J Clin Invest 1994;94:2493–2503. [PubMed: 7989608]
18. Thompson RW, Holmes DR, Mertens RA, Liao S, Botney MD, Mecham RP, Welgus HG, Parks WC. Production and localization of 92-kilodalton gelatinase in abdominal aortic aneurysms. An elastolytic metalloproteinase expressed by aneurysm-infiltrating macrophages. J Clin Invest 1995;96:318–326. [PubMed: 7615801]
19. Pyo R, Lee JK, Shipley JM, Curci JA, Mao D, Ziporin SJ, Ennis TL, Shapiro SD, Senior RM, Thompson RW. Targeted gene disruption of matrix metalloproteinase-9 (gelatinase B) suppresses development of experimental abdominal aortic aneurysms. J Clin Invest 2000;105:1641–1649. [PubMed: 10841523]
20. Ducharme A, Frantz S, Aikawa M, Rabkin E, Lindsey M, Rohde LE, Schoen FJ, Kelly RA, Werb Z, Libby P, Lee RT. Targeted deletion of matrix metalloproteinase-9 attenuates left ventricular enlargement and collagen accumulation after experimental myocardial infarction. J Clin Invest 2000;106:55–62. [PubMed: 10880048]
21. Mukherjee R, Brinsa TA, Dowdy KB, Scott AA, Baskin JM, Deschamps AM, Lowry AS, Escobar GP, Lucas DG, Yarbrough WM, Zile MR, Spinale FG. Myocardial infarct expansion and matrix metalloproteinase inhibition. Circulation 2003;107:618–625. [PubMed: 12566376]
22. Johnson C, Galis ZS. Matrix metalloproteinase-2 and -9 differentially regulate smooth muscle cell migration and cell-mediated collagen organization. Arterioscler Thromb Vasc Biol 2004;24:54–60. [PubMed: 14551157]
23. Mason DP, Kenagy RD, Hasenstab D, Bowen-Pope DF, Seifert RA, Coats S, Hawkins SM, Clowes AW. Matrix metalloproteinase-9 overexpression enhances vascular smooth muscle cell migration and alters remodeling in the injured rat carotid artery. Circ Res 1999;85:1179–1185. [PubMed: 10590245]
24. Cho A, Reidy MA. Matrix metalloproteinase-9 is necessary for the regulation of smooth muscle cell replication and migration after arterial injury. Circ Res 2002;91:845–851. [PubMed: 12411400]
25. Grabner R, Lotzer K, Dopping S, Hildner M, Radke D, Beer M, Spanbroek R, Lippert B, Reardon CA, Getz GS, Fu YX, Hehlgans T, Mebius RE, van der Wall M, Kruspe D, Englert C, Lovas A, Hu D, Randolph GJ, Weih F, Habenicht AJ. Lymphotoxin beta receptor signaling promotes tertiary lymphoid organogenesis in the aorta adventitia of aged ApoE-/- mice. J Exp Med 2009;206:233–248. [PubMed: 19139167]
26. Overall CM, Kleifeld O. Towards third generation matrix metalloproteinase inhibitors for cancer therapy. Br J Cancer 2006;94:941–946. [PubMed: 16538215]
27. Hudson MP, Armstrong PW, Ruzyllo W, Brum J, Cusmano L, Krzeski P, Lyon R, Quinones M, Theroux P, Sydlowski D, Kim HE, Garcia MJ, Jaber WA, Weaver WD. Effects of selective matrix

metalloproteinase inhibitor (PG-116800) to prevent ventricular remodeling after myocardial infarction: results of the PREMIER (Prevention of Myocardial Infarction Early Remodeling) trial. J Am Coll Cardiol 2006;48:15–20. [PubMed: 16814643]

28. Chen J, Tung CH, Allport JR, Chen S, Weissleder R, Huang PL. Near-infrared fluorescent imaging of matrix metalloproteinase activity after myocardial infarction. Circulation 2005;111:1800–1805. [PubMed: 15809374]
29. Deguchi JO, Aikawa M, Tung CH, Aikawa E, Kim DE, Ntziachristos V, Weissleder R, Libby P. Inflammation in atherosclerosis: visualizing matrix metalloproteinase action in macrophages in vivo. Circulation 2006;114:55–62. [PubMed: 16801460]
30. Chang K, Francis SA, Aikawa E, Figueiredo JL, Kohler RH, McCarthy JR, Weissleder R, Plutzky J, Jaffer FA. Pioglitazone suppresses inflammation in vivo in murine carotid atherosclerosis: novel detection by dual-target fluorescence molecular imaging. Arterioscler Thromb Vasc Biol 2010;30:1933–1939. [PubMed: 20689078]
31. Olson ES, Jiang T, Aguilera TA, Nguyen QT, Ellies LG, Scadeng M, Tsien RY. Activatable cell penetrating peptides linked to nanoparticles as dual probes for in vivo fluorescence and MR imaging of proteases. Proc Natl Acad Sci U S A 2010;107:4311–4316. [PubMed: 20160077]
32. Ohshima S, Fujimoto S, Petrov A, Nakagami H, Haider N, Zhou J, Tahara N, Osako MK, Fujimoto A, Zhu J, Murohara T, Edwards DS, Narula N, Wong ND, Chandrashekhar Y, Morishita R, Narula J. Effect of an antimicrobial agent on atherosclerotic plaques: assessment of metalloproteinase activity by molecular imaging. J Am Coll Cardiol 2010;55:1240–1249. [PubMed: 20298932]
33. Hwang AB, Franc BL, Gullberg GT, Hasegawa BH. Assessment of the sources of error affecting the quantitative accuracy of SPECT imaging in small animals. Phys Med Biol 2008;53:2233–2252. [PubMed: 18401059]

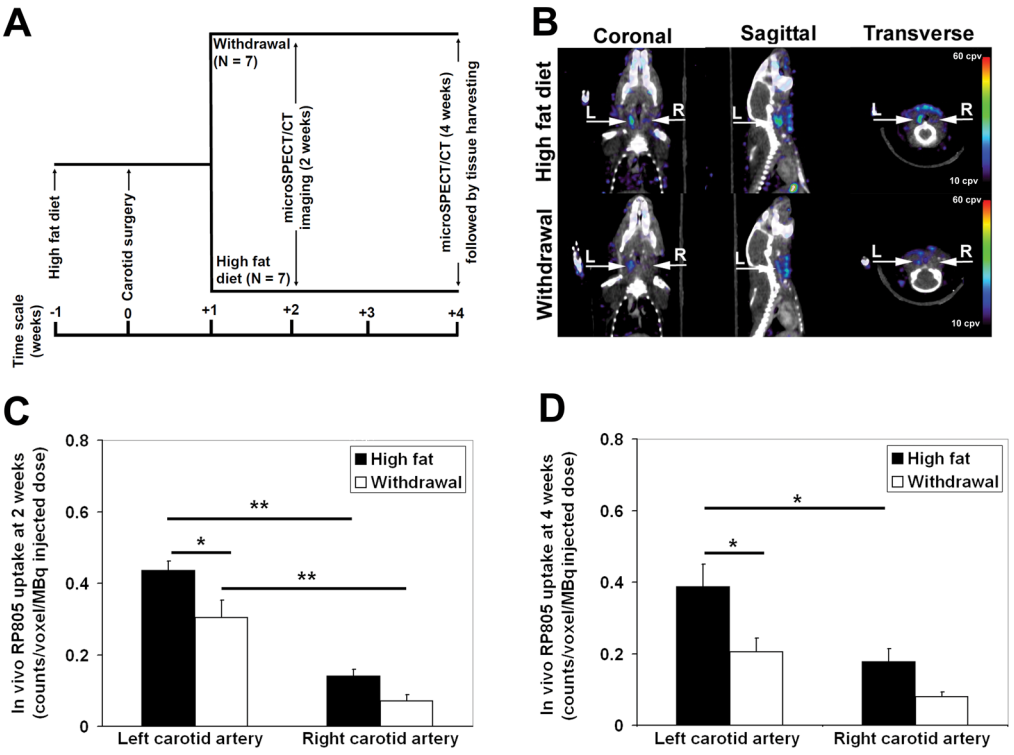


**Figure 1.**

**A,** Schematic presentation of the experimental design. **B,** Representative fused microSPECT and CT angiography images of mice two weeks after left common carotid artery wire injury demonstrating focal uptake of RP805 in injured arteries. Arrows point to left (L) and right (R) carotid arteries, cpv: counts per voxel. **C–D,** In vivo quantification of RP805 uptake in carotid arteries demonstrating a significant reduction in left carotid background-corrected RP805 uptake at 2 and 4 weeks after injury in the withdrawal group. * $P$ <0.05, ** $P$ <0.001.

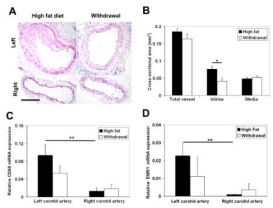


**Figure 2.**

**A,** Representative examples of hematoxylin and eosin staining, **B,** morphometric analysis and **C,** GAPDH-normalized CD68 and **D,** GAPDH-normalized EMR1 mRNA expression of sham-operated right, and injured left common carotid arteries in apoE$^{-/-}$ mice at 4 weeks after surgery. Scale bar: 100 μm. * $P$ <0.05, ** $P$ <0.01.

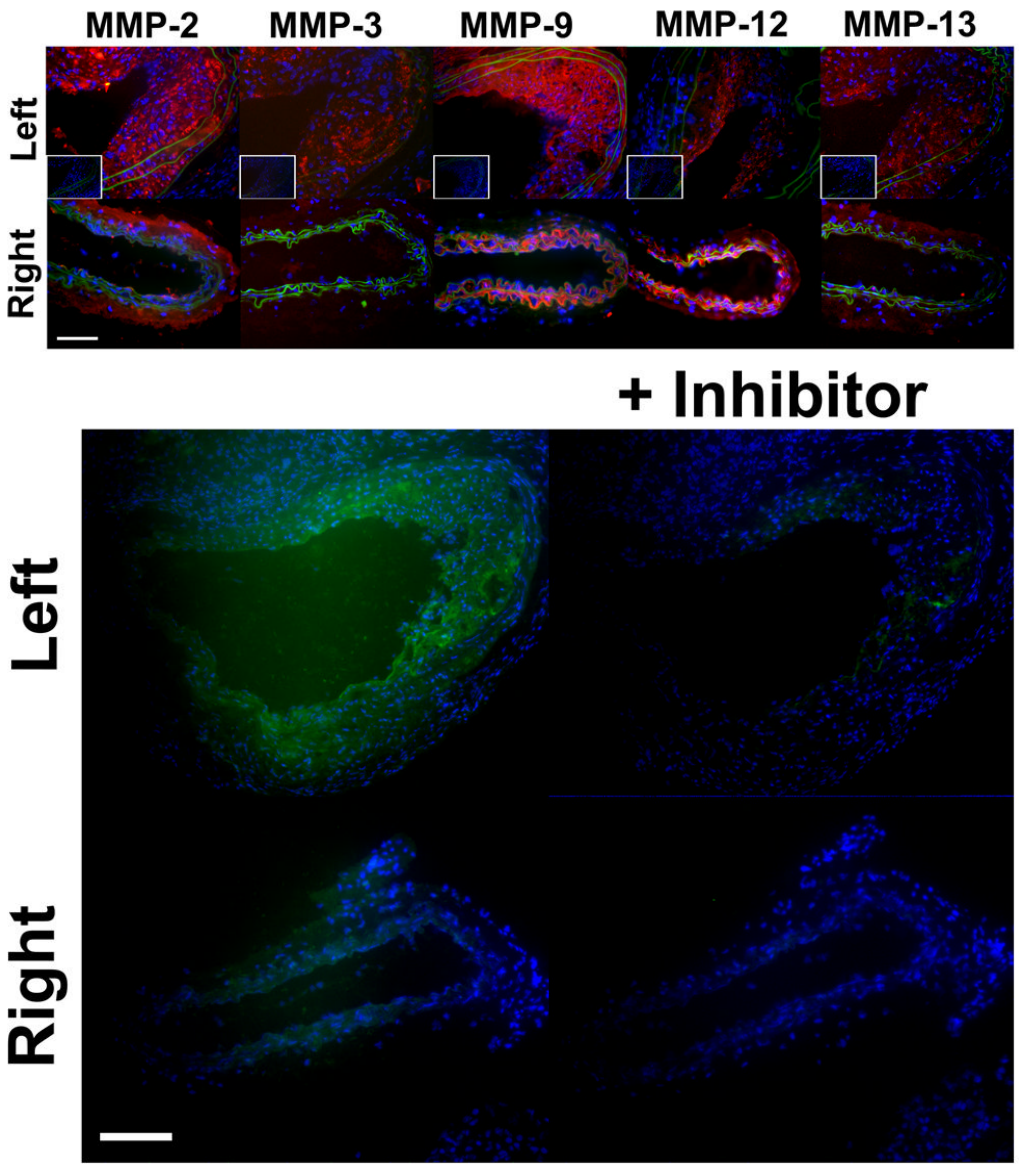


**Figure 3.**

**A,** Representative examples of MMP immunofluorescent staining (in red) of sham-operated right, and injured left common carotid arteries in apoE$^{-/-}$ mice at 4 weeks after surgery. Elastic membrane autofluorescence is in green and nuclei are stained with DAPI in blue. In sham-operated right carotid arteries, expression of MMP-2 (mainly in the adventitia), MMP-9 (mainly in the media), and MMP-12 (in both media and adventitia) are readily detectable, while MMP-3 and MMP-13 staining is negligible. In remodeling arteries, MMPs are diffusely expressed and predominantly localized in the neointima and media. The insets represent staining with control antibodies. Scale bar: 50 μm. **B,** Examples of in situ gelatinase activity (in green) in the absence or presence of an MMP inhibitor, 1,10-phenanthroline, in sham-operated right, and injured left common carotid arteries at 4 weeks after surgery. Nuclei are stained with DAPI in blue. Scale bar: 100 μm.

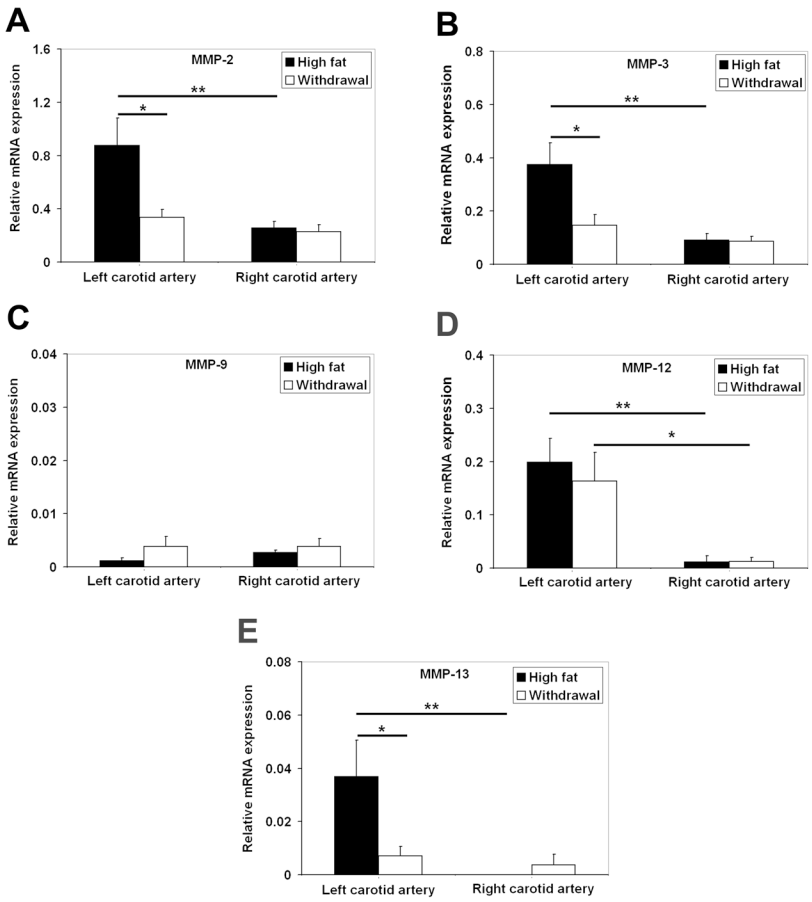


**Figure 4.**

**A–E,** GAPDH-normalized MMPs mRNA expression in the injured and sham-operated carotid arteries at 4 weeks after surgery demonstrating a reduction in MMP-2, MMP-3, and MMP-13 expression in animals withdrawn from the high fat diet (* $P$ <0.05, ** $P$ <0.01).

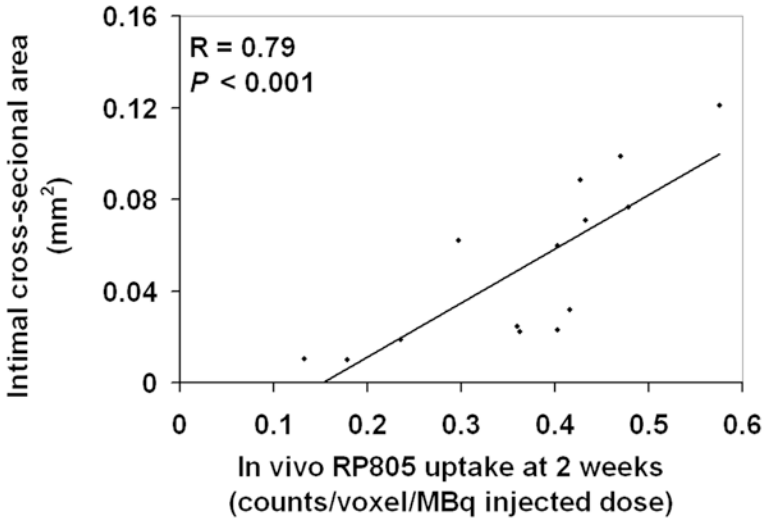


**Figure 5.**
Correlation between left carotid RP805 uptake on in vivo microSPECT/CT images at 2 weeks after injury and neointimal cross-sectional area in the same arteries at 4 weeks after injury.

**Table 1**

Correlation between RP805 uptake and GAPDH-normalized CD68, EMR1 and MMP mRNA expression at 4 weeks after surgery

| | R | *P* |
|---|---|---|
| CD68 | 0.67 | < 0.001 |
| EMR1 | 0.57 | < 0.05 |
| MMP-2 | 0.55 | < 0.01 |
| MMP-3 | 0.66 | < 0.01 |
| MMP-9 | 0.22 | NS |
| MMP-12 | 0.30 | NS |
| MMP-13 | 0.64 | < 0.01 |

MMP: matrix metalloproteinase; NS: not significant